ACS APPLIED MATERIALS & INTERFACES

RESEARCH ARTICLE

www.acsami.org

Hydrophobic but Hygroscopic Polymer Films — Identifying Interfacial Species and Understanding Water Ingress Behavior

Erik Hsiao, Anna L. Barnette, Laura C. Bradley, and Seong H. Kim*

Department of Chemical Engineering and Materials Research Institute, The Pennsylvania State University, University Park, Pennsylvania 16802, United States

ABSTRACT: The hydrophobic but hygroscopic nature of polydimethylsiloxane (PDMS) with quaternary ammonium cationic side chains adsorbed on a SiO_2 surface was investigated with sum frequency generation vibration spectroscopy (SFG) and attenuated total reflectance infrared spectroscopy (ATR-IR). PDMS with cationic side chains, named cationic polymer lubricant (CPL), forms a self-healing boundary lubrication film on SiO_2. It is interesting that CPL films are externally hydrophobic but internally hydrophilic. The comparison of SFG and ATR-IR data revealed that the methyl groups of the PDMS backbone are exposed at the film/air interface and the cationic side groups and counterions are embedded within the film. The hydrophobicity must originate from the surface CH_3 groups, while the ionic groups inside the film must be responsible for water uptake. The surface hydrophobicity can alleviate the capillary adhesion while the hygroscopic property enhances the mobility and self-healing capability of the CPL boundary lubrication film.

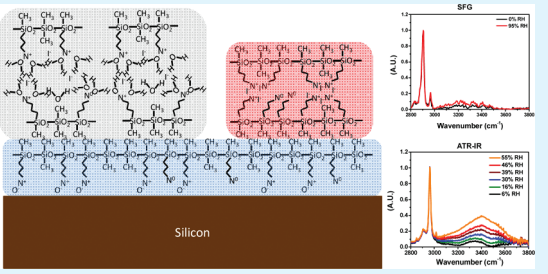

KEYWORDS: boundary lubricant layer, water adsorption, ATR-IR, SFG, hydrophobicity, hygroscopicity

1. INTRODUCTION

Humidity in ambient air is the major contributor that increases adhesion and wear in silicon-based microdevices such as microelectromechanical systems (MEMS).[1,2] In humid environments, the adsorbed water layer on the surface causes capillary adhesion at interfaces and induces tribochemical wear of the sliding interfaces.[2−4] Thus, it is vital to prevent water from reaching the SiO_2 surface by treating the surface with hydrophobic and lubricious organic coatings. Many organic surface modifiers and polymers with low surface energies can be used for this purpose.[5−7] Probably, the most widely studied example is self-assembled monolayers (SAMs).[8,9] However, the SAM protective layer can be damaged easily under sliding conditions.[8,9] Because the thickness of SAMs is self-limited to a monolayer covalently bonded to the surface, there are no excess molecules in the film, which can migrate and self-heal the damaged area.

One can overcome this drawback by coating the surface with a bound-and-mobile lubrication film with self-healing capability. Polydimethylsiloxane (PDMS) with quaternary ammonium cationic side chains, called cationic polymer lubricant (CPL), has recently been shown to form such film on SiO_2.[10−12] The CPL film is hydrophobic; water contact angle is higher than 90°. So, the 'water adsorption' on the CPL film from air is energetically unfavorable. Usually, such films have negligible humidity dependence in their lubrication performance.[13−15] However, the performance of CPL films is humidity dependent. Surprisingly, the humidity improves the lubrication performance of CPL, opposite to what was expected. The self-healing behavior of CPL was enhanced by ~25% in humid environment when compared to dry conditions.[11] This was thought to be due to "water absorption" into the film. But, the water penetration to the interior of the film did not cause the tribochemical wear of the underlying SiO_2 substrate. So, it is an interesting interfacial problem to understand how the CPL film exhibits the surface hydrophobicity, allows water absorption, and protects the underlying substrate from chemical wear.

In this paper, the CPL film structure was studied with sum frequency generation (SFG) spectroscopy and attenuated total reflection infrared (ATR-IR) spectroscopy to understand how the CPL film shows hydrophobicity and hygroscopicity that are seemingly exclusive to each other. SFG is a nonlinear vibration spectroscopy that is sensitive to detect organic functional groups at the film/air interface. ATR-IR can provide the functional groups present in the entire film. The comparison of SFG and ATR-IR analysis results revealed that the CPL film surface is terminated with CH_3 groups rendering surface hydrophobicity, and the ionic groups interacting with water are present within the film. The hygroscopicity of ionic groups enhances the self-healing capabilities of CPL in humid ambient and their strong electrostatic binding to the surface makes CPL capable of preventing humidity's detrimental tribochemical wear of SiO_2 surfaces.

2. EXPERIMENTAL DETAILS

A detailed description of the CPL synthesis was reported elsewhere.[10,11,16] In brief, poly(methylhydrosiloxane-co-dimethylsiloxane) was hydrosilylated with N,N-dimethylallyl amine with a PtO_2 catalyst at 50 °C. The product was then reacted with methyl iodide to produce the

Received: July 7, 2011
Accepted: October 21, 2011
Published: October 21, 2011

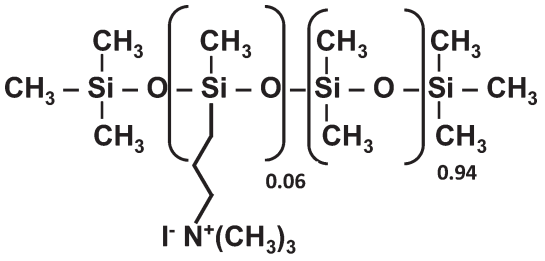

Figure 1. Chemical structure of cationic polymer lubricant (CPL).

quaternary ammonium iodide cationic groups as shown in Figure 1. The poly(methylhydrosiloxane-co-dimethylsiloxane) random copolymer with a molecular weight of ~2000 g/mol was obtained from Gelest with methylhydrosiloxane mole percents of 6%. N,N-dimethylallyl amine was obtained from Sigma-Aldrich. Methyl iodide and PtO_2 were obtained from Alfa Aesar. A 2000 g/mol molecular weight PDMS was purchased from Gelest as a control to compare with CPL.

Static water contact angles were measured with an automated First Ten Angstrom goniometer. A 10 μL droplet of Milli-Q water was placed in the focus point of a magnifying camera to measure the static water contact angle. The fused quartz windows were immersed in a KOH bath for 5 min followed by a RCA-1 process (5:1:1 mixture in Mill-Q water, 30% ammonium hydroxide, and 30% hydrogen peroxide at 70 °C). An ethanol−water (1:9) solution containing 1.0 wt-% of 6% CPL was spun at a speed of 3000 rpm producing a film thickness of ~4.0 nm (ellipsometry − Ellipsotech SWE; wavelength = 632.8 nm, incidence angle = 70°). In addition, 2000 g/mol PDMS was also coated onto the cleaned quartz window for comparison with CPL. PDMS was spin-coated from a 0.1 wt % PDMS in chloroform solution, giving a film thickness of ~4.0 nm.

To observe the friction, wear, and self-healing capabilities of CPL, a pin-on-disk tribometer was used. This pin-on-disk tribometer is home built and the details can be found elsewhere.[10,11] A 3 mm SiO_2 ball rubbing against silicon at an applied load of 0.5 N, a Hertzian contact diameter of 50 μm, was used to measure friction. A load cell gauge calibrated with known weights was used to measure the friction force. Using Amonton's law, the friction coefficient can be calculated. Wear can be observed on the ball and substrate with an optical microscope. Self-healing was observed by changing the time between cycles to allow enough time for lateral spreading to self-heal.

The polymer/air interface was probed with Visible+IR SFG vibration spectroscopy. Our SFG system used an EKSPLA optical parametric generator/amplifier (OPG/OPA) pumped by an EKSPLA picosecond Nd:Yag laser at a 10 Hz repetition rate. A combination of β-BaB_2O_4 and $AgGaS_2$ crystal was used to generate a tunable IR between 2−10 μm and the second harmonic of the Nd:Yag laser produced visible light at 532 nm. The visible and IR beams are overlapped in time and space to generate the SFG photon. The incident angle of the IR and visible light were 56° and 60° from the surface normal, respectively. The hydrocarbon stretching vibration region (2800−3000 cm^{-1}) was collected at 4 cm^{-1} steps and the hydroxyl stretching vibration region (3000−3800 cm^{-1}) was collected at 8 cm^{-1} steps. Each point is the average of 100 shots. All experiments were performed with the s (for SFG signal), s (for visible), and p (for IR) polarization combination.

ATR-IR was performed using a Thermo Nicolet Nexus 670 spectrometer equipped with a mercury cadmium telluride (MCT) detector to measure the water uptake of CPL. A silicon ATR crystal with a 45° angle of incidence and a total of 11 internal reflections was used in this study. The silicon ATR crystal was cleaned for 30 min in a piranha solution (3:1 concentrated sulfuric acid and 30% hydrogen peroxide at room temperature) followed by 30 min with a RCA-1 process. This cleaning method hydroxylates the ~2 nm thick native SiO_2 layer. The 6% CPL

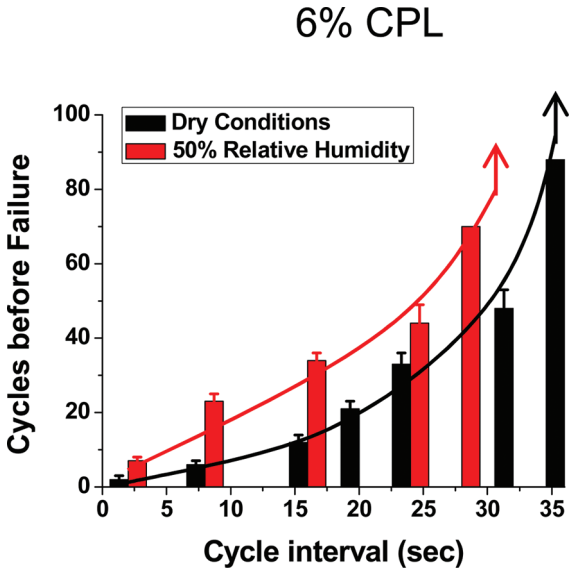

Figure 2. Performance of 6% CPL as a function of cycle interval at dry conditions and 50% relative humidity. The lateral spreading rate in dry condition was estimated to be 2.0 × 10^{-11} m^2/s and at 50% relative humidity to be 2.5 × 10^{-11} m^2/s.

films were deposited on the ATR crystal by spin coating. An ethanol−water (1:9) solution containing 1.0 wt-% of 6% CPL was spun at a speed of 3000 rpm producing a film thickness of ~4.0 nm. After CPL was coated onto the ATR crystal, dry argon was flowed for 2 h to ensure a dry CPL background. The humidity was controlled by mixing a dry Ar stream and a water-vapor-saturated Ar stream at varying ratios.

The effective thickness of the water layers was estimated using thin film theory.[17] This method was previously discussed in detail.[18,19] In brief, the refractive indices of water (~1.3) and silicon (~3.45) were used to determine the penetration depth of the IR beam into the water from the ATR crystal as a function of wavenumber. The bulk liquid spectra were used in conjunction with the penetration depth to determine the absorbance per unit path length. The absorbance per unit path length was assumed to be constant for the adsorbed/absorbed water layers. The effective thickness of the thin water layers was estimated from ratio the adsorbed water spectra intensities between ~3400−3500 cm^{-1} and the absorbance per unit path length. The results of these calculations were compared with previous experimental results for water adsorption on silicon.[18]

3. RESULTS AND DISCUSSIONS

CPL has shown to coat SiO_2 on silicon wafers and to reduce adhesion, friction, and wear significantly compared to the bare SiO_2 surface. CPL reduces adhesion from 500 nN to ~50 nN.[10] CPL also provides a friction coefficient (~0.2) significantly lower than the bare SiO_2 surface (>0.6). In addition, CPL has been shown to self-heal through lateral spreading.[11] Figure 2 shows the number of cycles for which the ~4 nm thick CPL film lubricated the SiO_2 surface before it failed and allowed the substrate wear. Without CPL coating, the wear of bare SiO_2 starts after the first cycle. As the interval between consecutive cycles was increased, the CPL film in the slide region (~50 μm wide) has more time to self-heal through lateral flow from outside the slide contact region; thus, the same thickness film can provide lubrication for longer periods of time. The number of operation cycles before failure could be analyzed with simple one-dimensional diffusion model to estimate the lateral spreading rate. The 4 nm CPL film

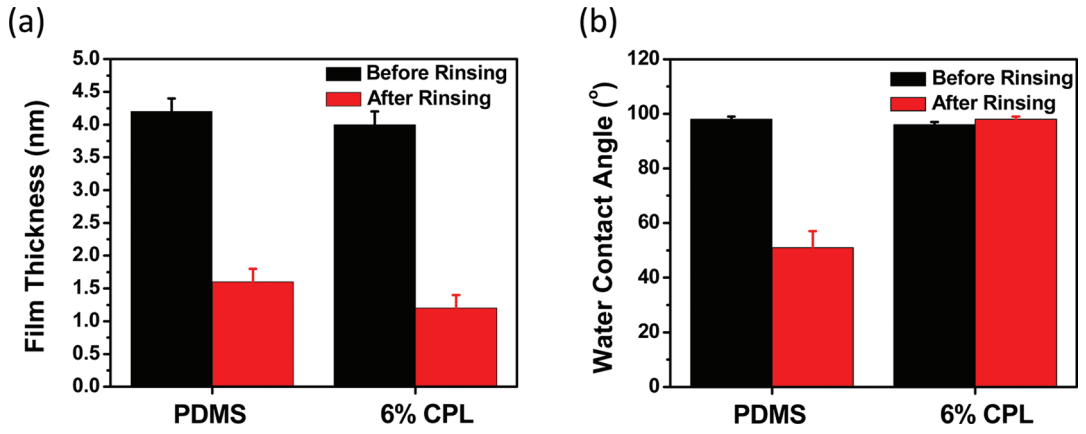

Figure 3. (a) Film thickness measured before and after thoroughly rinsing with water for a 2000 g/mol PDMS and 6% CPL films on silicon wafer and (b) static water contact angles before and after thoroughly rinsing with water for a 2000 g/mol PDMS and 6% CPL films on silicon wafer.

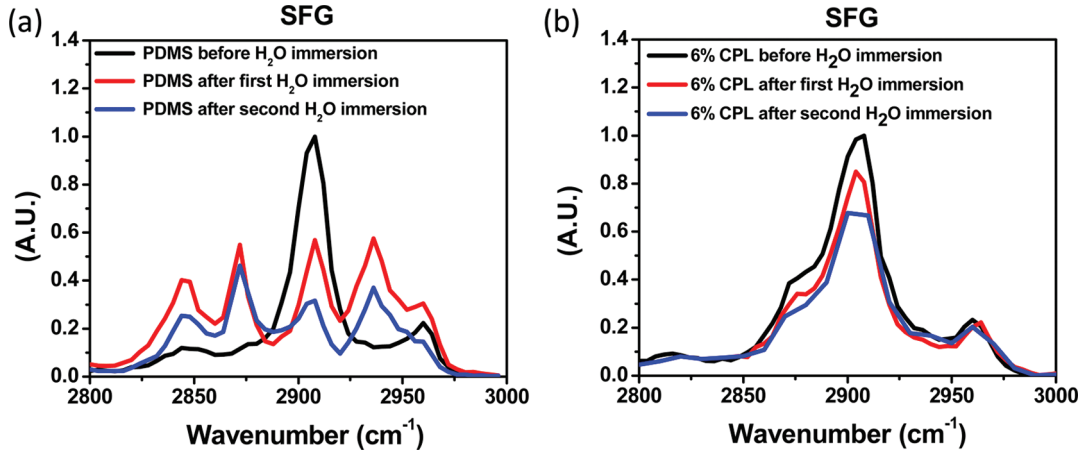

Figure 4. SFG spectra of the polymer/air interface before and after immersion in water twice for (a) 2000 g/mol PDMS and (b) 6% CPL.

shows a lateral spreading rate of $2.0 \pm 0.2 \times 10^{-11}$ m^2/s in dry conditions and $2.5 \pm 0.2 \times 10^{-11}$ m^2/s in 50% relative humidity conditions.[11,12] Therefore, humidity enhances CPL's self-healing capabilities.

On SiO_2, the 4 nm thick CPL film consists of a bound monolayer and mobile multilayers. The mobile multilayer is formed over the 1.2 nm thick monolayer, which is bound to the substrate through ionic interactions.[10,11] If this film is thoroughly rinsed with a good solvent such as water or alcohol, the multilayer is completely removed and only the bound layer remains as shown in Figure 3a. This remaining film was previously analyzed with X-ray photoelectron spectroscopy (XPS). About 30% of the quaternary ammonium groups are reduced to ternary amines.[12] The film remaining after rinsing contains no I^- counter-anions although it still has cationic groups (N^+), indicating that the 1.2 nm thick CPL monolayer is electrostatically bound to the negatively charged silicon oxide surface. This strongly bound layer plays an important role in lubricating and protecting SiO_2 surface. The CPL multilayer has a hydrophobic property with a water contact angle of 98° and the bound layer also has a hydrophobic water contact angle of ~95° as shown in Figure 3b. The hydrophobicity of the CPL monolayer bound to SiO_2 prevents the detrimental effects of humidity on the SiO_2 wear.

The water contact angle and rinsing behaviors of PDMS with the same molecular weight, but without cationic side chains, was analyzed for comparison with CPL. Because PDMS is neutral, it is weakly bound to the SiO_2 surface via van der Waals and can easily be displaced. When the PDMS film is thoroughly rinsed with water, ellipsometry measures a 1.6 nm thick film remaining on SiO_2 (Figure 3a). However, ellipsometry alone cannot tell what this remaining film is. This 1.6 nm thick remaining layer is not hydrophobic. After rinsing with water, the static water contact angle is reduced from ~98° (highly hydrophobic) to ~50° (partially hydrophilic).

The air/polymer/substrate interfaces of the CPL and PDMS films were analyzed with SFG to obtain molecular insights into the surface hydrophobicity. Figure 4a shows the SFG spectra for the substrate/PDMS/air interface before and after immersion in Milli-Q water. Before immersion, the C−H stretch region of the PDMS spectrum shows the symmetric (2908 cm^{-1}) and asymmetric (2960 cm^{-1}) vibration of the CH_3 group in the PDMS backbone.[1,20−26] The CH_3 symmetric stretching peak is much larger than the CH_3 asymmetric stretching peak, which is consistent with the previously reported SFG spectra of the air/PDMS interface. At the air/polymer interface, the CH_3 of the PDMS backbone is oriented close to the direction perpendicular to the polymer/air interface.[1,20−23,25] This complements the

water contact angle measurement of water of ~98°, rendering the surface hydrophobic.

After immersion of the PDMS film in water, the SFG spectra of the remaining film have drastically changed. The Si-CH_3 symmetric stretching peak from the PDMS backbone at 2908 cm^{-1} has decreased; at the same time three peaks at 2844, 2876, and 2936 cm^{-1} grow significantly.[20−24,26] These peaks could be attributed to organic contaminants because they cannot be assigned to the Si-CH_3 group of PDMS. This could mean that the PDMS layer is partially dewetted after immersion in water and the newly exposed substrate surface is covered with organic contaminants. The organic contamination is believed to arise from exposing the dewetted substrate surface to air after immersion in water. Water can easily penetrate the interface between the clean hydrophilic silicon oxide substrate and the hydrophobic PDMS film. The dewetting of PDMS must be responsible for the reduced static water contact angle (~50°) after rinsing with water. The decrease in the intensity ratio of the 2908 and 2960 cm^{-1} peaks could be attributed to two possibilities. In the first case, the average orientation of methyl groups changes from being predominantly perpendicular to the surface interface for the fully covered flat film (water contact angle of 98°) to less ordered or widely distributed within the dewetted patchy film (water contact angle of 50°). The second case is that the peaks from the contaminants from the air superimpose the SFG spectra of PDMS. It is difficult to distinguish between contaminant peaks superimposing PDMS peaks in SFG.

Figure 4b shows the SFG spectra for substrate/CPL/air interface before and after immersion in water. The CH_3 symmetric stretching and CH_3 asymmetric stretching peaks from CPL's PDMS backbone at 2908 and 2960 cm^{-1}, respectively, can be seen as dominant peaks. A shoulder centered at 2876 cm^{-1} may be attributed to the CH_3 symmetric stretching peak from the methyl group attached to the ammonium cationic group.[1,20−26] Similar to the substrate/PDMS/air spectra before immersion in water, the Si-CH_3 symmetric stretching in the CPL spectra is much larger than the Si-CH_3 asymmetric stretching. This suggests that the CH_3 groups of the CPL's PDMS backbone are oriented perpendicular to the interface. The surface energy of the methyl group (~21 mJ/m) is lower than the ionic groups and the water contact angle of the CPL film is the same as that of the PDMS film (Figure 3b). Thus, it is concluded that the methyl groups of the polymer backbone are exposed at the CPL/air interface and the methyl groups of the cationic side chain in the bound layer face toward the substrate. After immersion in water twice, it is clear that the surface structure of the 1.2 nm thick monolayer of CPL remaining on the surface is the same as that of the CPL multilayer. It is believed that this is due to the strong electrostatic interactions between the quaternary ammonium ions and the SiO_2 surface, which prevents dewetting of the film and protects the surface from ingression of water. The termination of both multilayers and bound monolayer surfaces with the CH_3 group of the PDMS backbone explains the hydrophobicity of these film surfaces with water contact angles higher than 90°.

Comparison of SFG and ATR-IR spectra obtained in humid gas environments explains how the CPL film can be hydrophobic yet still hygroscopic. Figure 5a shows the SFG spectra of CPL/air interface in dry condition and at 95% relative humidity. The O−H intensity of the SFG spectra of the ~4.0 nm thick CPL film is very weak and does not change in dry and 95% relative humidity gas environments. The O−H peak must be due to water molecules trapped at the CPL/substrate interface, solvating ionic groups.

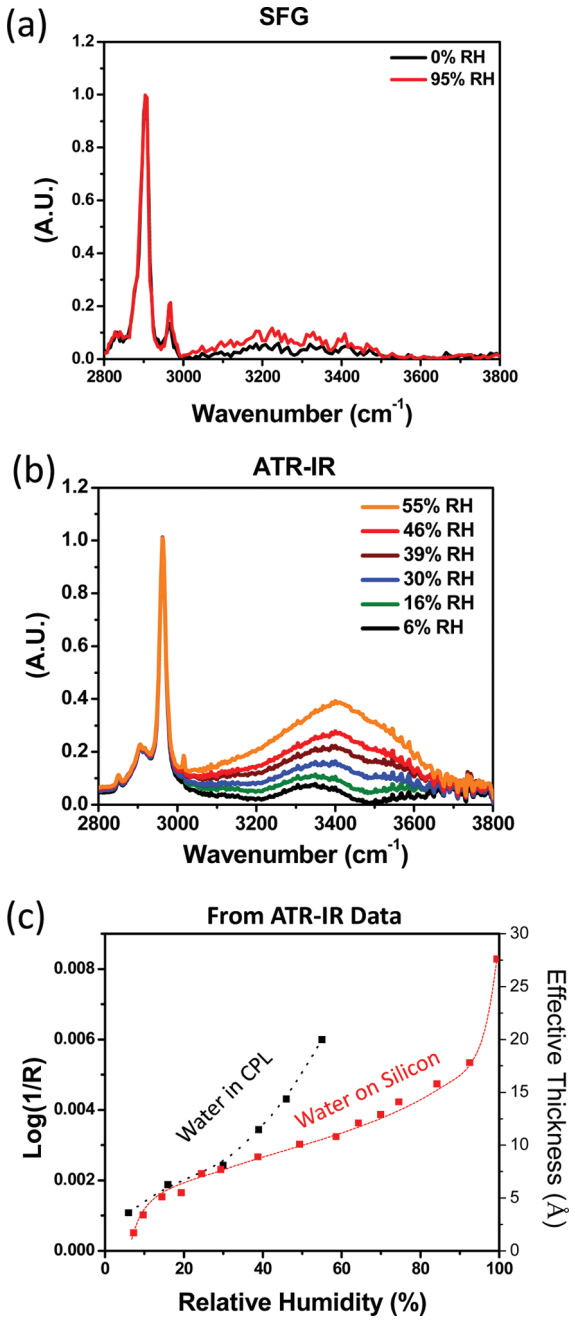

Figure 5. (a) SFG spectra at the CPL/air interface at dry and 95% relative humidity, (b) ATR-IR spectra at various relative humidity of 6% CPL, and (c) effective water thickness from ATR-IR data for water absorption into 6% CPL and water adsorption on silicon.

The weak signal implies that they are not well-ordered. Because the CPL layer is terminated with hydrophobic methyl groups (water contact angle = 98°), it is very unlikely that water adsorbs at the CPL/air interface. The adsorption of water on the CH_3-terminated surface is energetically unfavorable since it will result in the increase in surface energy. The SFG spectra in Figure 5a shows a slight increase in intensity for the broad peak observed in the OH vibration region when the RH was increased to near saturation conditions (~95% RH). However, it is difficult to distinguish whether this is due to the increase in water content or ordering at the CPL/substrate.

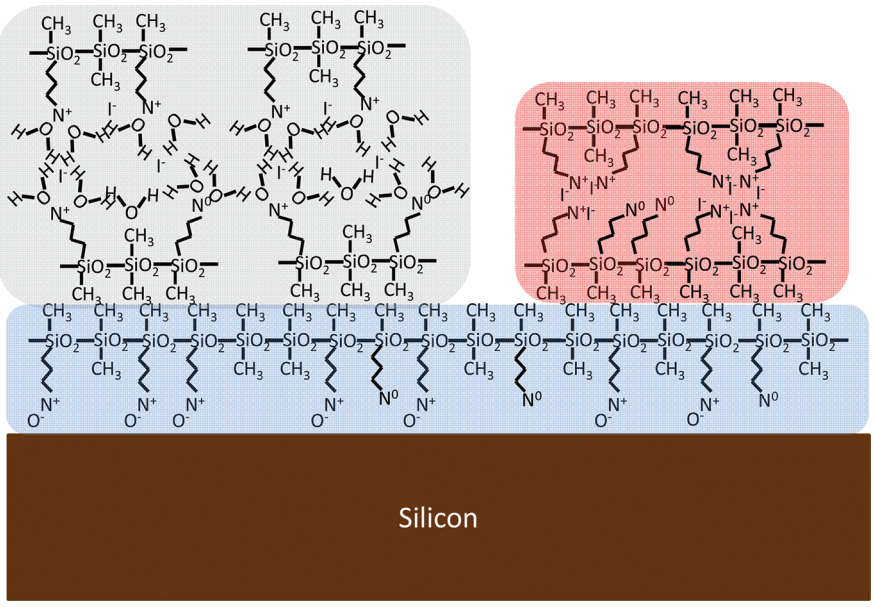

Figure 6. Schematic of water absorption into CPL on silicon. There is an electrostatically bound layer (0.8 nm thick) followed by a hydrophobic multilayer with bimodal distribution due to dipole−dipole interactions (2.5 nm thick). Water absorbs into the CPL film interacting with the cationic groups in the multilayer, increasing the film by ~1.2 nm at 50% relative humidity. It should also be noted that 30% of the quaternary ammonium cations (N^+) are reduced to neutral species (N^0).

Although no water molecule in the vapor phase can adsorb on the CPL film surface, the water molecule can penetrate into the bulk film. A similar behavior has been observed for highly hydrophobic octadecylsiloxane (OTS) SAMs on SiO_2.[27,28] The water uptake of CPL was probed with ATR-IR. Figure 5b shows ATR-IR spectra of CPL film (~4.0 nm thick) in various relative humidity environments. The ATR-IR spectra shows the symmetric and asymmetric CH_3 stretching vibrations from the Si-CH_3 groups are 2906 and 2962 cm^{-1}, respectively. In IR, the asymmetric CH_2 peak is much stronger than the symmetric peak. The CH_2 symmetric stretching of the propyl linker group appears at 2850 cm^{-1}. Additionally there is the CH_3 asymmetric stretch of the quaternary ammonium cations at 3010 cm^{-1}. As humidity increases, the OH stretching peak at ~3350 cm^{-1} grows first and then the 3400 cm^{-1} OH peak becomes dominant at high relative humidity. The 3400 cm^{-1} peak corresponds to liquid water. The 3350 cm^{-1} OH peak corresponds to a more highly hydrogen bonded water than the 3400 cm^{-1} OH peak; but it is not fully hydrogen-bonded as in the solid-like water (~3250 cm^{-1}).[18,29] The lack of growth in the OH vibration in SFG and the growth of OH vibration observed in ATR are clear evidence that water absorbed into the CPL film; thus, the CPL film is hygroscopic.

Figure 5c shows the effective thickness of the absorbed water uptaken inside the CPL film estimated from the 3400 cm^{-1} intensity at a given relative humidity. This was compared with the water adsorption isotherm data on bare SiO_2 surface in Figure 5c.[18] The water uptake into the CPL film is estimated to be ~1.5 nm at 50% relative humidity. It is noteworthy that this water is accommodated inside the CPL film, while the SiO_2 surface is still protected from water by the electrostatically bound CPL layer.

Based on the SFG and ATR-IR measurements, the structure of the CPL film can be represented with a schematic shown in Figure 6. Overlayers are formed on an electrostatically bound layer (~1 nm thick). The interaction between the first and second layer is mostly van der Waals interactions since the first layer is terminated with CH_3 groups. This may inevitably expose high-energy ionic groups at the second layer surface. To minimize the surface energy, another CPL layer could form to cover the ionic groups and expose the low-energy CH_3 group again.[30,31] This could produce a bimodal thickness distribution, i.e., patches of one- and three-layer thicknesses, instead of a homogeneous two-layer thick film. In fact, such a thickness distribution was observed for the CPL multilayer film in noncontact atomic force microscopy imaging in a previous study.[10,11] The water molecules can penetrate into the CPL film and interact with the ionic groups inside the CPL film (Figure 5c). However, the CPL/air interface is still terminated with the Si-CH_3 groups rendering the surface hydrophobic and the CPL/substrate interface is occupied by the cationic side group interacting with the negatively charged SiO_2 surface.

CONCLUSION

CPL is a hydrophobic film on SiO_2, but also has a hygroscopic nature. SFG and ATR-IR gave molecular insights into how CPL can have these seemingly opposite properties. The methyl groups from the PDMS backbone of CPL are exposed at the CPL/air. In multilayer CPL films, the cationic groups and counterions are present inside the polymer film and interact with water molecules that penetrate into the film. The CPL/substrate interface contains only cationic groups interacting electrostatically with the substrate surface preventing the detrimental wear effects of humidity on SiO_2.

AUTHOR INFORMATION

Corresponding Author

*E-mail: shkim@engr.psu.edu.

■ ACKNOWLEDGMENT

This work was supported by the National Science Foundation (CMS-0637028 and CMMI-0625493).

■ REFERENCES

(1) Kim, J.; Opdahl, A.; Chou, K. C.; Somorjai, G. A. *Langmuir* **2003**, *19* (23), 9551–9553.
(2) Patton, S. T.; Cowan, W. D.; Eapen, K. C.; Zabinski, J. S. *Tribol. Lett.* **2000**, *9* (3−4), 199–209.
(3) Barnette, A. L.; Asay, D. B.; Kim, D.; Guyer, B. D.; Lim, H.; Janik, M. J.; Kim, S. H. *Langmuir* **2009**, *25* (22), 13052–13061.
(4) Zanoria, E. S.; Danyluk, S.; McNallan, M. J. *Tribol. Trans.* **1995**, *38* (3), 721–727.
(5) Israelachvili, J. N., *Intermolecular and Surface Forces*; Academic Press: San Diego, CA, 1992.
(6) Schmaucks, G.; Sonnek, G.; Wustneck, R.; Herbst, M.; Ramm, M. *Langmuir* **1992**, *8* (7), 1724–1730.
(7) Vogler, E. A. *Adv. Colloid Interface Sci.* **1998**, *74*, 69–117.
(8) Ashurst, W. R.; Yau, C.; Carraro, C.; Maboudian, R.; Dugger, M. T. *J. Microelectromech. Syst.* **2001**, *10* (1), 41–49.
(9) Linford, M. R.; Fenter, P.; Eisenberger, P. M.; Chidsey, C. E. D. *J. Am. Chem. Soc.* **1995**, *117* (11), 3145–3155.
(10) Hsiao, E.; Kim, D.; Kim, S. H. *Langmuir* **2009**, *25* (17), 9814–9823.
(11) Hsiao, E.; Bradley, L.; Kim, S. *Tribol. Lett.* **2011**, *41* (1), 33–40.
(12) Hsiao, E.; Veres, B. D.; Tudryn, G. J.; Kim, S. H. *Langmuir* **2011**, *27* (11), 6808–6813.
(13) Bhushan, B.; Liu, H. W.; Hsu, S. M. *J. Tribol.* **2004**, *126* (3), 583–590.
(14) Tao, Z.; Bhushan, B. *Tribol. Lett.* **2006**, *21* (1), 1–16.
(15) Ashurst, W. R.; Yau, C.; Carraro, C.; Lee, C.; Kluth, G. J.; Howe, R. T.; Maboudian, R. *Sens. Actuators, A* **2001**, *91* (3), 239–248.
(16) Sabourault, N.; Mignani, G.; Wagner, A.; Mioskowski, C. *Org. Lett.* **2002**, *4* (13), 2117–2119.
(17) Harrick, N. *Attenuated Total Reflectance Spectroscopy of Polymers*; American Chemical Society: Washington D.C., 1996.
(18) Asay, D. B.; Kim, S. H. *J. Phys. Chem. B* **2005**, *109* (35), 16760–16763.
(19) Barnette, A. L.; Asay, D. B.; Janik, M. J.; Kim, S. H. *J. Phys. Chem. C* **2009**, *113* (24), 10632–10641.
(20) Liu, Y.; Messmer, M. C. *J. Phys. Chem. B* **2003**, *107* (36), 9774–9779.
(21) Opdahl, A.; Koffas, T. S.; Amitay-Sadovsky, E.; Kim, J.; Somorjai, G. A. *J. Phys.: Condens. Matter* **2004**, *16* (21), R659–R677.
(22) Wang, J.; Paszti, Z.; Even, M. A.; Chen, Z. *J. Am. Chem. Soc.* **2002**, *124* (24), 7016–7023.
(23) Wang, J.; Woodcock, S. E.; Buck, S. M.; Chen, C. Y.; Chen, Z. *J. Am. Chem. Soc.* **2001**, *123* (38), 9470–9471.
(24) Chen, C. Y.; Loch, C. L.; Wang, J.; Chen, Z. *J. Phys. Chem. B* **2003**, *107* (38), 10440–10445.
(25) Clarke, M. L.; Chen, C. Y.; Wang, J.; Chen, Z. *Langmuir* **2006**, *22* (21), 8800–8806.
(26) Chen, C. Y.; Wang, J.; Chen, Z. *Langmuir* **2004**, *20* (23), 10186–10193.
(27) Du, Q.; Freysz, E.; Shen, Y. R. *Science* **1994**, *264* (5160), 826–828.
(28) Ye, S.; Nihonyanagi, S.; Uosaki, K. *Phys. Chem. Chem. Phys.* **2001**, *3* (16), 3463–3469.
(29) Barnette, A. L.; Asay, D. B.; Kim, S. H. *Phys. Chem. Chem. Phys.* **2008**, *10* (32), 4981–4986.
(30) Ma, X.; Gui, J.; Smoliar, L.; Grannen, K.; Marchon, B.; Jhon, M. S.; Bauer, C. L. *J. Chem. Phys.* **1999**, *110* (6), 3129–3137.
(31) Ma, X.; Gui, J.; Smoliar, L.; Grannen, K.; Marchon, B.; Bauer, C. L.; Jhon, M. S. *Phys. Rev. E* **1999**, *59* (1), 722–727.